

^{124}Te AND THE E(5) CRITICAL POINT SYMMETRY

D. G. GHIȚĂ^{*,†}, G. CĂȚA-DANIL^{*,†}, D. BUCURESCU^{*},
I. CĂȚA-DANIL^{*}, M. IVASCU^{*}, C. MIHAI^{*},
G. SULIMAN^{*}, L. STROE^{*}, T. SAVA^{*} and N. V. ZAMFIR^{*}

^{*}*Horia Hulubei National Institute for Physics and Nuclear Engineering,
Bucharest-Magurele, Romania*

[†]*Physics Department, University Politehnica of Bucharest, Romania*

Received 13 March 2008

Revised 15 May 2008

We present a new study of the low-lying states in ^{124}Te nucleus by γ -ray spectroscopy following $^{124}\text{I} \beta^+/\varepsilon$ decay. The β radioactive sources were produced in the $^{124}\text{Te}(p, n)^{124}\text{I}$ reaction induced by 11 MeV protons, delivered by the Bucharest FN Tandem Accelerator. The γ -rays were measured in a low background area with three large volume HPGe detectors. A total number of 276 million double coincidence events were recorded in a six-day run. Most of the gamma line intensities previously measured were confirmed with improved accuracy and several gamma lines were obtained for the first time. Our results, combined with those from a recent (n, γ) study are compared with the predictions of the E(5) critical point symmetry model and numerical IBA-1 model calculations at the critical point of the U(5)–O(6) phase transition.

Keywords: β decay; γ transitions; level energies; collective models.

PACS Number(s): 23.40.-s, 23.20. Lv, 27.60.+j, 21.60.Ev

1. Introduction

During the last decades, the low-lying structure of the ^{124}Te isotope has been the testing ground for various nuclear collective models and especially for various developments of the Interaction Boson Model (IBA).¹ From the numerical diagonalization of the full IBA-1 and IBA-2 Hamiltonians excitation energies, electromagnetic transition probabilities, and two nucleon transfer reaction strengths have been obtained and compared with the experimental values.^{2,3} None of these studies provided a detailed description of *all* spectroscopic properties when a single collective configuration was involved. The possibility of the occurrence of low-lying intruder states in nuclei with $A \approx 130$ requires more sophisticated theoretical descriptions. Thus, by mixing two IBA-2 collective configurations theoretical results were able to better describe the experimental data, although at the expense of a larger number of model parameters.^{4,5}

From the point of view of the dynamical symmetries of the IBA-1 model, previous studies⁴ placed the ^{124}Te nuclear structure on the leg U(5) (spherical vibrator) to O(6) (deformed γ soft) of the symmetry triangle.⁶ Robinson *et al.*⁷ concluded that there are several reasons to associate the structure of ^{124}Te with the theoretical O(6) symmetry, although there are some gamma transitions outside the predictions of this dynamical symmetry limit. In a later study, Lee *et al.*⁸ suggested also that ^{124}Te may be a good example of an O(6) nucleus.

A significant step in understanding nuclear symmetries was achieved by Iachello with the introduction of the critical point symmetry concept.^{9,10} The critical shape phase transition point X(5) is located on the U(5)–SU(3) leg of the symmetry triangle and it was observed experimentally for the first time in the ^{152}Sm nucleus.¹¹ The critical point of the phase transition between the U(5) and O(6) dynamical symmetries defines the E(5) symmetry⁹ and it was experimentally identified for the first time in ^{134}Ba ¹² and ^{102}Pd .¹³

A systematic search for the E(5) candidate nuclei by Clark *et al.*¹⁴ was based on significant structure indicators such as energy ratios and B(E2) ratios which involve the 2_1^+ , 4_1^+ , 0_2^+ and 0_3^+ levels.

This study concludes that the structure of the ^{124}Te nucleus has several E(5) features, although not as clear as other proposed candidates, such as ^{128}Xe and ^{134}Ba . Recently Mihai *et al.*¹⁵ systematically searched for the E(5) structure based on the analysis of the $R_{4/2} = E_{4_1^+}/E_{2_1^+}$ ratio and the staggering factor $S_4 = [(E_{4_1^+} - E_{3_1^+}) - (E_{3_1^+} - E_{2_1^+})]/E_{2_1^+}$ in the quasi- γ band. Typical E(5) values for these indicators are $R_{4/2} = 2.20$ and $S_4 = -1.39$. This general search did not indicate ^{124}Te as an E(5) candidate. It was later observed that the search in Ref. 15 was performed on the basis of the adopted levels in the ENSDF database,¹⁶ which did not include the results of newer experiments. Indeed, the subsequent paper of Warr *et al.*² proposed a 2^+ , 3^+ doublet at 2039 keV, based on the comparison of the (α , 2n) experiment with the ^{129}I decay one (see also references in this work to previous studies which pointed out a possible doublet at this energy), while an ultra-high resolution experiment performed with the GAMS crystal spectrometer at ILL Grenoble⁵ clearly evidenced this doublet, separated by only 0.13 keV, and the decay of its states. With the 2039 keV 3^+ state, one now gets $S_4 = -1.34$, a value which is very close to the E(5) value of -1.39 (and also brings ^{124}Te in the range of S_4 values of the other Te isotopes¹⁵). This observation re-opened the question as to whether one can find additional evidence about the possible E(5) structure of this nucleus.

The ^{124}Te nucleus was investigated by various reactions which provided an almost complete level scheme up to an excitation energy of 3–4 MeV. The most recent references are the study by (n, γ), (γ , γ'), and transfer reactions with light projectiles,³ beta decay and the (α , 2n γ) reaction,² precise γ -ray spectroscopy with a crystal spectrometer⁵ and an extensive (n, γ) study.¹⁷

In the present paper we approach the issue of the presence of E(5) features in the low-lying structure of the ^{124}Te nucleus through a new experiment and a detailed

phenomenological analysis. We performed new γ -ray spectroscopy measurements in ^{124}Te following the β^+/ε decay of ^{124}I , with the purpose of obtaining more accurate weak branching ratios. These data, together with previous information, are then compared with the analytical predictions of the $E(5)$ model and with numerical IBA-1 model calculations at the critical point of the $U(5)$ – $O(6)$ phase transition.¹⁸

2. Experiment

The low-lying states of ^{124}Te were populated in the β^+/ε decay of the 2^- ground state of ^{124}I ($T_{1/2} = 4.1760$ d). The parent nuclei were produced in the $^{124}\text{Te}(p, n)^{124}\text{I}$ reaction. We used a thick tellurium oxide target, enriched 90% in the ^{124}Te isotope. A proton beam with an intensity of 5 nA was delivered by the Bucharest FN Tandem accelerator. The energy of the protons was 11 MeV in order to optimize the production of ^{124}I below the opening of the $(p, 2n)$ reaction channel. Gamma lines following β^+/ε decay were measured off-beam by means of γ -ray spectroscopy.

Taking advantage of the long lifetime of the 2^- ground state of ^{124}I , the activity collected in the target after about eight hours of beam exposure was transferred to a low background measurement site. Three HPGe detectors with efficiencies of about 25% were used to detect the γ radiation from the target in singles and coincidence modes. Single spectra and two-fold $\gamma\gamma$ coincidence data were accumulated during a six-day run by using two targets and an alternating procedure of irradiation and measuring each one. The counting rate on each detector reached 8 kHz at the beginning of the measuring cycle. The relative detection efficiency curve and the

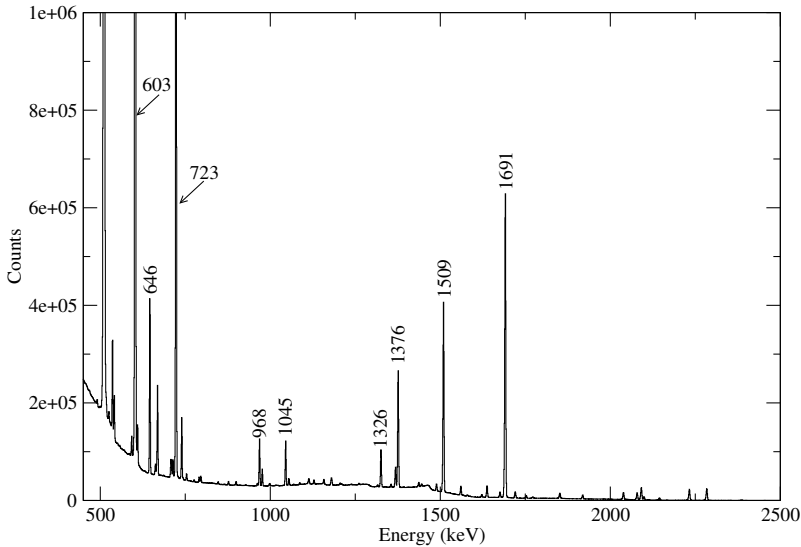


Fig. 1. Total projection spectrum of the symmetric matrix. The most intense γ lines of ^{124}Te are labeled with their energies.

Table 1. γ rays assigned to ^{124}Te from the present experiment. J^π values are taken from Refs. 17 and 19. Intensities are obtained from singles and/or γ - γ coincidences and are normalized to 100 for the 602 keV $2_1^+ \rightarrow 0_1^+$ transition.

Energy (keV)	Relative intensity	E_i (keV)	J_i^π	E_f (keV)	J_f^π
306.6(1)	0.020(4)	3001.0	3^-	2693.7	3^-
335.3(1)	0.027(9)	2293.7	3^-	1957.9	4^+
350.8(1)	0.016(4)	2834.9	3^-	2483.2	3^+
364.2(2) ^a	0.003(2)	2886.1	3^-	2521.2	2^+
370.4(2) ^b	0.004(2)	2693.7	3^-	2322.9	2^+
378.7(5) ^a	0.002(1)	2701.5	2^-	2322.9	2^+
402.2(2)	0.018(7)	2886.1	3^-	2483.2	3^+
443.8(1) ^d	<0.006	2483.2	3^+	2039.4	2^+
443.8(1) ^d	<0.041	2483.2	3^+	2039.3	3^+
468.5(2) ^b	0.012(7)	2693.7	3^-	2224.9	4^+
490.9(3) ^{b,c}	0.045(5)	2945.6	2^+	2454.0	2^+
517.6(1)	0.030(10)	3001.0	3^-	2483.2	3^+
525.3(1)	0.033(5)	2483.2	3^+	1957.9	4^+
541.1(1)	0.321(5)	2834.9	3^-	2293.7	3^-
557.5(1)	0.065(10)	1882.8	0^+	1325.5	2^+
571.0(1)	0.016(10)	2454.0	2^+	1882.8	0^+
592.4(5)	0.171(4)	2886.1	3^-	2293.7	3^-
602.7(1)	100	602.7	2^+	0	0^+
609.8(3)	0.232(4)	2834.9	3^-	2224.9	4^+
632.7(6) ^b	0.005(1)	1957.9	4^+	1325.5	2^+
645.9(1)	1.556(5)	1248.5	4^+	602.7	2^+
661.1(1) ^a	0.018(3)	2886.1	3^-	2224.9	4^+
662.3(1)	0.083(10)	2701.5	2^-	2039.3	3^+
678.3(1) ^b	0.006(2)	3001.0	3^-	2322.9	2^+
707.5(1)	0.146(3)	3001.0	3^-	2293.7	3^-
709.3(1)	0.069(3)	1957.9	4^+	1248.5	4^+
713.8(2) ^d	<0.003 ^e	2039.4	2^+	1325.5	2^+
713.8(2) ^d	<0.120 ^e	2039.3	3^+	1325.5	2^+
722.8(1)	16.325(13)	1325.5	2^+	602.7	2^+
735.8(1) ^b	0.021(12)	2693.7	3^-	1957.9	4^+
743.3(1)	0.021(4)	2834.9	3^-	2091.5	2^+
776.4(1)	0.021(3)	3001.0	3^-	2224.9	4^+
790.8(1) ^d	<0.37 ^e	2039.4	2^+	1248.5	4^+
790.8(1) ^d	<0.05 ^e	2039.3	3^+	1248.5	4^+
794.7(3) ^a	0.004(1)	2886.1	3^-	2091.5	2^+
795.7(1) ^d	<0.064	2834.9	3^-	2039.4	2^+
795.7(1) ^d	<0.064	2834.9	3^-	2039.3	3^+
797.1(1) ^b	0.006(3)	2454.0	2^+	1657.3	0^+
846.8(1) ^d	<0.004	2886.1	3^-	2039.4	2^+
846.8(1) ^d	<0.004	2886.1	3^-	2039.3	3^+
877.1(1)	0.035(3)	2834.9	3^-	1957.9	4^+
899.6(1)	0.035(3)	2224.9	4^+	1325.5	2^+
962.2(1)	0.030(3)	3001.0	3^-	2039.3	3^+
968.3(1)	0.704(5)	2293.7	3^-	1325.5	2^+
976.5(1)	0.147(4)	2224.9	4^+	1248.5	4^+
998.3(1) ^a	0.041(3)	2322.9	2^+	1325.5	2^+
1045.2(1)	0.677(5)	2293.7	3^-	1248.5	4^+

Table 1. (Continued).

Energy (keV)	Relative intensity	E_i (keV)	J_i^π	E_f (keV)	J_f^π
1054.8(1)	0.196(4)	1657.3	0 ⁺	602.7	2 ⁺
1086.5(1) ^{b,c}	0.025(4)	2335.1	5 ⁻	1248.5	4 ⁺
1128.7(1)	0.076(5)	2454.0	2 ⁺	1325.5	2 ⁺
1195.6(1)	0.003(2)	2521.2	2 ⁺	1325.5	2 ⁺
1205.8(1)	0.049(4)	2454.0	2 ⁺	1248.5	4 ⁺
1234.2(1)	0.004(2)	2483.2	3 ⁺	1248.5	4 ⁺
1315.8(1)	0.044(4)	2641.1	2 ⁺	1325.5	2 ⁺
1325.6(1)	2.535(9)	1325.5	2 ⁺	0	0 ⁺
1355.3(1)	0.054(5)	1957.9	4 ⁺	602.7	2 ⁺
1368.2(1)	0.465(6)	2693.7	3 ⁻	1325.5	2 ⁺
1376.1(1)	2.826(10)	2701.5	2 ⁻	1325.5	2 ⁺
1392.7(1) ^a	0.023(5)	2641.1	2 ⁺	1248.5	4 ⁺
1436.6(1) ^d	<0.057 ^e	2039.4	2 ⁺	602.7	2 ⁺
1436.6(1) ^d	<0.122 ^e	2039.3	3 ⁺	602.7	2 ⁺
1445.2(1)	0.051(5)	2693.7	3 ⁻	1248.5	4 ⁺
1488.9(1)	0.314(5)	2091.5	2 ⁺	602.7	2 ⁺
1509.4(1)	5.115(11)	2834.9	3 ⁻	1325.5	2 ⁺
1560.6(1)	0.219(24)	2886.1	3 ⁻	1325.5	2 ⁺
1622.2(1)	0.069(3)	2224.9	4 ⁺	602.7	2 ⁺
1637.5(1)	0.316(4)	2886.1	3 ⁻	1248.5	4 ⁺
1663.7(1) ^a	0.004(1)	2988.3	2 ⁺	1325.5	2 ⁺
1675.7(4)	0.162(4)	3001.0	3 ⁻	1325.5	2 ⁺
1691.0(1)	17.607(20)	2293.7	3 ⁻	602.7	2 ⁺
1720.5(1)	0.321(6)	2322.9	2 ⁺	602.7	2 ⁺
1752.7(1)	0.080(3)	3001.0	3 ⁻	1248.5	4 ⁺
1851.5(1)	0.341(4)	2454.0	2 ⁺	602.7	2 ⁺
1918.7(1)	0.261(4)	2521.2	2 ⁺	602.7	2 ⁺
2038.6(1)	0.539(4)	2641.1	2 ⁺	602.7	2 ⁺
2091.1(2)	0.946(5)	2693.7	3 ⁻	602.7	2 ⁺
2099.1(1)	0.239(3)	2701.5	2 ⁻	602.7	2 ⁺
2144.5(1)	0.161(2)	2747.1	1 ⁻	602.7	2 ⁺
2214.8(7) ^{a,c}	0.009(1)	2817.4	2 ⁺	602.7	2 ⁺
2232.3(1)	0.954(21)	2834.9	3 ⁻	602.7	2 ⁺
2256.7(8) ^{b,c}	0.005(2)	2859.1	2 ⁺	602.7	2 ⁺
2283.5(2)	1.032(5)	2886.1	3 ⁻	602.7	2 ⁺
2385.5(2)	0.028(1)	2988.3	2 ⁺	602.7	2 ⁺

^aNew γ -ray transition.

^bObserved for the first time in β^+/ε decay.

^cDeexcites a level observed for the first time in β^+/ε decay.

^dUnresolved doublet; individual γ -rays and 2039.3 and 2039.4 keV level energies as reported in Refs. 5 and 17.

^eObtained using the branching ratios from Ref. 17.

energy calibration were obtained by measuring standard ^{152}Eu and ^{56}Co calibration sources.

Coincidence data were recorded in list-mode and sorted into $\gamma\gamma$ coincidence matrices by using a 45 ns gate on the time spectra. The all-detector symmetric matrix, constructed with the GASPWARE software package, contained 2.76×10^8

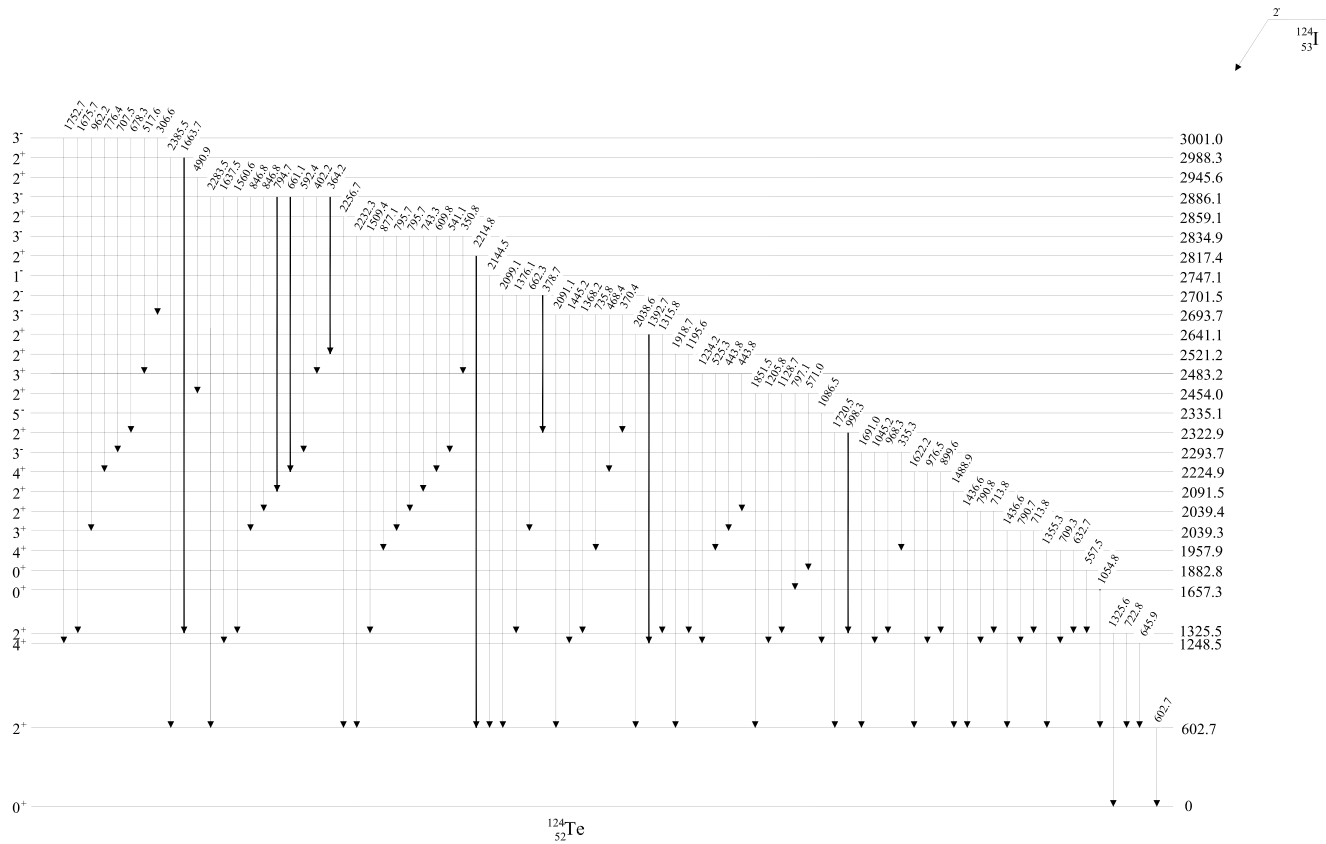


Fig. 2. Experimental level scheme of ^{124}Te as obtained in the present experiment. Up to 1656 keV excitation energy, the level positions are proportional to their excitation energies and above are equally spaced. Newly observed γ -ray transitions are represented by thicker arrows. The J^π values are taken from Ref. 17, except those for the 2817 and 2859 keV levels (see text).

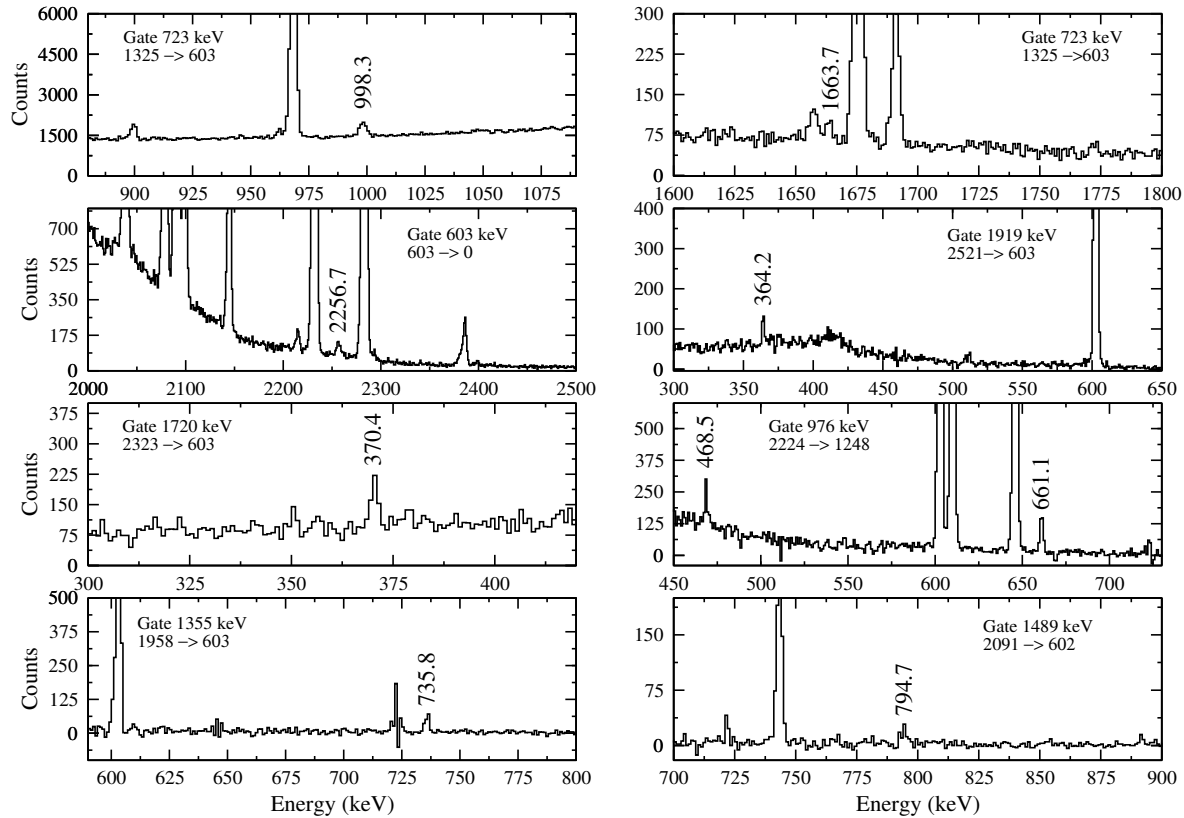


Fig. 3. Gated γ -ray spectra illustrating new γ -ray transitions in ^{124}Te observed for the first time in the present experiment. These transitions are labeled with their energies, and the energies of the levels between which the gated transition takes place ($E_{\text{initial}} \rightarrow E_{\text{final}}$) are indicated on each graph.

Table 2. The $\log ft$ values resulting from the present measurements. They are calculated with the relative intensities from Table 1 and compared with the $\log ft$ values from Refs. 2 and 16.

E_{level} keV	J^π	$\log ft$ (present work)	$\log ft$ (from Ref. 2)	$\log ft$ (from Ref. 16)
0	0 ⁺	9.27(4)	9.27(4)	9.27
602.7	2 ⁺	7.5(1)	7.5(1)	7.49
1248.5	4 ⁺	10.1(1)	10.2(4)	—
1325.5	2 ⁺	7.9(1)	7.9(1)	7.86
1657.3	0 ⁺	10.3(1)	9.4(1)	10.3
1882.8	0 ⁺	9.8(2)	10.4(6)	—
1957.9	4 ⁺	10.3(1)	10.0(5)	—
2039.3	3 ⁺	<9.3	9.7(2) ^a	—
2039.4	2 ⁺	<9.3	9.7(2) ^a	—
2091.5	2 ⁺	8.7(1)	8.9(1)	8.82
2224.9	4 ⁺	—	10.0(1)	—
2293.7	3 ⁻	6.9(1)	6.9(1)	6.88
2322.9	2 ⁺	8.6(1)	8.7(1)	8.66
2335.1	5 ⁻	9.7(1)	9.8(1)	—
2454.0	2 ⁺	8.3(1)	—	8.20
2483.2	3 ⁺	9.6(6)	—	8.81
2521.2	2 ⁺	8.4(1)	—	8.44
2641.1	2 ⁺	7.9(1)	—	7.86
2693.7	3 ⁻	7.4(1)	—	7.41
2701.5	2 ⁻	7.0(1)	—	7.06
2747.1	1 ⁻	7.5(1)	—	7.49
2817.4	2 ⁺	9.3(2)	—	—
2834.9	3 ⁻	6.4(1)	—	6.43
2859.1	2 ⁺	9.4(3)	—	—
2886.1	3 ⁻	6.8(1)	—	6.81
2988.3	2 ⁺	8.1(1)	—	7.96
3001.0	3 ⁻	6.8(1)	—	6.82

^a The $\log ft$ value calculated for the 2039 keV level as an unresolved doublet in Refs. 2 and 16.

coincidence events. The average energy resolution on the total projection spectrum of the symmetric matrix was 2.6 keV for 1 MeV gamma photons.

Weak transitions were observed from the symmetric matrix, which contains the full statistics of the experiment. Asymmetric matrices were also constructed for each pair of detectors and were used for extracting information on the relative intensities. Figure 1 presents the total projection of the symmetric matrix, where the strong gamma lines of the ^{124}Te nucleus are indicated.

The list of gamma lines observed in the present experiment, with their measured relative intensities, is presented in Table 1. Intensities are normalized to the 602 keV $2_1^+ \rightarrow 0_1^+$ transition.

Figure 2 presents the experimental level scheme constructed on the basis of our experiment. Three energy levels known from previous experiments¹⁷ were seen for the first time in the β -decay: 2817, 2859 and 2946 keV. Newly observed γ -ray transitions (see Table 1) are represented with thicker arrows in this figure. Figure 3

illustrates these new γ transitions by appropriate gated spectra. In addition, some other transitions known from previous experiments were seen for the first time in the β -decay (see Table 1). For the 2817 and 2859 keV states now seen in β -decay we have adopted an assignment $J^\pi = 2^+$ as resulting from a recent measurement with a (p, t) reaction.¹⁹

New $\log ft$ values were calculated from the present experimental data, combined with additional information on the electromagnetic decay scheme from Ref. 17. Thus, for the levels at 2091, 2293, 2335, 2454, 2747, 2817, 2859, 2988 and 3001, for which we observed only the strongest transitions, we have added the weaker branches from Ref. 17. On the other hand, in the case of levels at 2694, 2701, 2835 and 2886 keV we have observed a larger number of branches. Also, in calculating the $\log ft$ values we assumed, as in Refs. 2 and 16 that the ground state is fed by 34.9% of the decay. The new $\log ft$ values are given in Table 2. There is good agreement between the values given in Table 2 and those from Ref. 2.

3. Discussion

With 52 protons and 72 neutrons, ¹²⁴Te is located close to $Z = 50$ and relatively far from $N = 82$ shell closure. The significant valence space for the low-lying collective excitation is generated by two particle-like protons ($N_\pi = 1$ bosons in the IBA picture) and ten hole-like neutrons ($N_\nu = 5$ bosons). This small to medium size valence space could accommodate vibrational²⁰ and gamma-soft⁷ structures, locating this nucleus (from the point of view of collective excitations) on the U(5) to O(6) leg of the IBA symmetry triangle. With the collectivity indicator $E_{4_1^+}/E_{2_1^+} = 2.072$ close to the vibrational limit of 2.0, this nucleus has many features of the simple quadrupole vibrator model. Indeed, the 4_1^+ state at 1248.6 keV and 2_2^+ at 1325.5 keV are possible members of the two phonon multiplet (the one phonon state 2_1^+ is located at 602.7 keV). However, the 0_2^+ state, which would then be expected to be the third member of the two-phonon multiplet, is located 408.7 keV higher in energy relative to 4_1^+ , indicating a significant anharmonicity.

A more precise localization of the ¹²⁴Te collective structure was suggested by Clark *et al.*¹⁴ in the framework of the proposed E(5) model of critical point symmetry. This picture of the nuclear excitation involves an analytical solution of the Bohr collective Hamiltonian with an infinite square well potential depending only on the quadrupole parameter β . In the E(5) model the quantum states are labeled by two numbers ξ and τ related to zeros of the Bessel functions.¹⁰ The quantum number ξ labels the principal families of the E(5) states and τ labels the phonon-like excitation within a given ξ family. A graphical representation of the level scheme calculated for the E(5) symmetry is presented in the middle panel of Fig. 4. An alternative description can be obtained in the framework of the IBA-1 model. The U(5)–O(6) transition is described by the Hamiltonian¹:

$$H = \varepsilon \hat{n}_d + AP^\dagger P,$$

where $\hat{n}_d = d^\dagger d$ represents the d -boson number operator and $P = 1/2[s \cdot s - \tilde{d} \cdot \tilde{d}]$. In this parametrization the critical point is defined by the ratio $\varepsilon/A = 2(N_B - 1)$, as given in Ref. 18, where $N_B = 6$ is the number of bosons in ^{124}Te . The E2 transitions are described by the operator

$$T(\text{E2}) = e_2[(s^\dagger \tilde{d} + d^\dagger s) + \chi(d^\dagger \tilde{d})],$$

where e_2 is the boson effective charge. The transition strengths were calculated with the parameter $\chi = -\sqrt{7}/2$ and normalized to the experimental value $B(\text{E2}, 2_1^+ \rightarrow 0_1^+) = 30$ W.u. corresponding to the effective charge $e_2 = 0.11$ eb. With the model parameters at the critical point $\varepsilon = 1$ and $A = 0.1$, the level scheme presented in the right-hand panel of Fig. 4 was obtained.

The left-hand panel of Fig. 4 presents the experimental level scheme of ^{124}Te , to be compared with the theoretical model predictions given in the other two panels. In the experimental level scheme the γ -ray transitions are labeled by the absolute $B(\text{E2})$ values, in Weisskopf units. When these values were either poorly known or not known, we give relative values (numbers marked by a star-symbol), which were calculated from the branching ratios. This is the case for the decay of the 4_2^+ level [in this case we have used the measured value $\delta(\text{E2/M1}) = -0.18$ (see Ref. 16) for the $4_2^+ \rightarrow 4_1^+$ transition], and for the 3_1^+ level, for which we assumed that all the decays are pure E2 transitions; for the sake of comparison, for these two levels we give the relative $B(\text{E2})$ values (marked by a star symbol) also for the calculated level schemes.

During the present experiment, only one transition was detected in the decay of the 0_3^+ state at 1882 keV. In a previous study⁵ this transition was determined to have a $B(\text{E2}, 0_3^+ \rightarrow 2_2^+) = 365$ W.u. but the measurement has a very large uncertainty (299 W.u.). The $B(\text{E2})$ values predicted by the theoretical calculations for the 0_ξ^+ state are only slightly smaller than the lower limit of the experimental ones. Also, the model predictions for the 0_ξ^+ state describe well the experimental decay pattern, with a much higher transition strength for the $0_3^+ \rightarrow 2_2^+$ branch, compared to the $0_3^+ \rightarrow 2_1^+$ one. Thus, we may assign this state as a member of the multiplet ($\xi = 1, \tau = 3$) in the E(5) picture.

The 0_2^+ state at 1657 keV has a decay pattern resembling that of the calculated 0_2^+ state from the ($\xi = 2, \tau = 0$) multiplet of the E(5) model. This state decays mainly to the 2_1^+ state with a $B(\text{E2}) = 19$ W.u., close to the model predictions, as can be observed in Fig. 4.

The 2_2^+ state at 1325 keV decays by a strong $B(\text{E2})$ transition to the 2_1^+ state [$B(\text{E2}, 2_2^+ \rightarrow 2_1^+) = 55$ W.u.] and a weak one to the ground state [$B(\text{E2}, 2_2^+ \rightarrow 0_1^+) = 0.4$ W.u.]. From these decay characteristics, the 2_2^+ state is clearly a member of the ($\xi = 1, \tau = 2$) multiplet of the E(5) scheme. Its characteristics are reasonably well described by the two theoretical calculations presented in Fig. 4.

For some of the γ transitions in the decay of the 4_2^+ and 3_1^+ states, there are measured only upper limits for the $B(\text{E2})$ values.⁵ From the measured gamma transition intensities, and assuming a pure quadrupole character of the transitions where

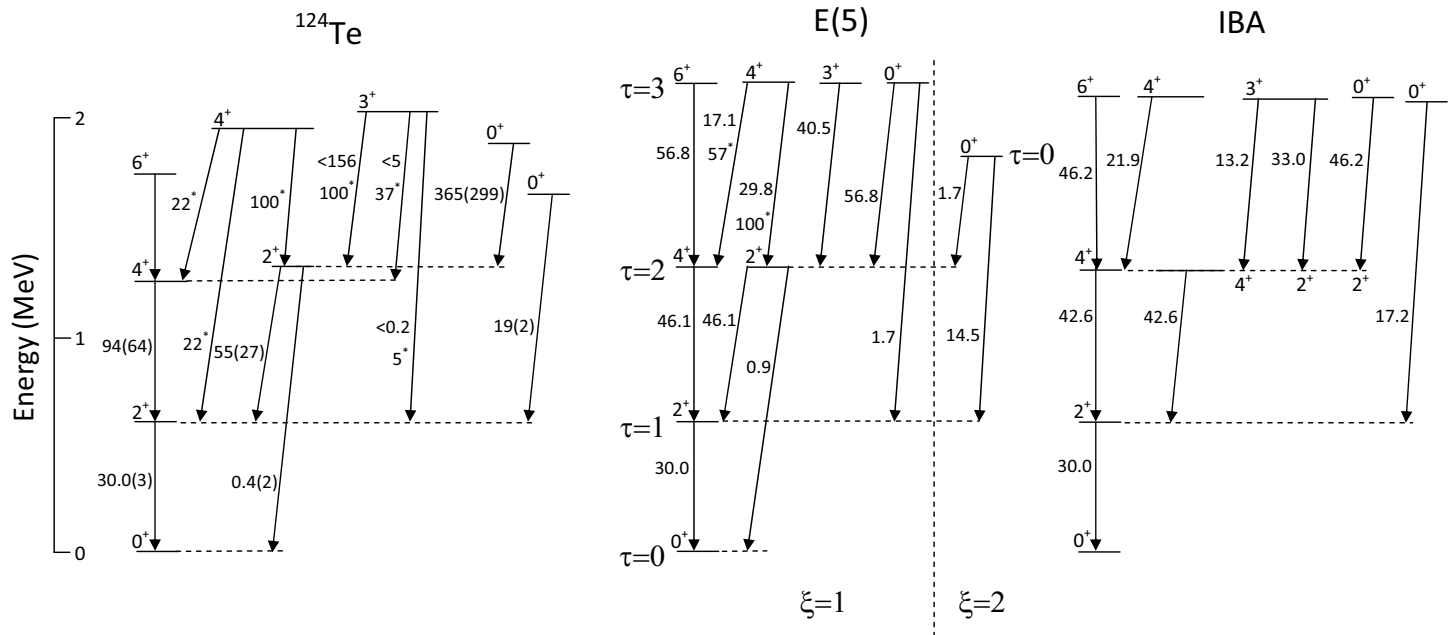


Fig. 4. ^{124}Te experimental level scheme compared with the E(5) and U(5)-O(6) critical point predictions (see text). The γ -decay transitions are labeled with their $B(E2)$ values. When experimental $B(E2)$ values were not known, relative $B(E2)$ values, marked with a star (with the biggest normalized to 100), were determined from the experimental branchings (see text for details).

mixing ratios were not known, we calculated the relative B(E2) values, indicated by star symbol in the left-hand panel of Fig. 4.

Experimentally, it is observed that the 4_2^+ state decays to the members of the ($\xi = 1, \tau = 2$) doublet and to the ($\xi = 1, \tau = 1$) singlet. The relative B(E2) values for these transitions are 100 (for $4_2^+ \rightarrow 2_2^+$), 22 (for $4_2^+ \rightarrow 4_1^+$), and 22 (for $4_2^+ \rightarrow 2_1^+$), respectively. The E(5) model predicts relative values of 100, 57, and very small, respectively, for the same three transitions, while the IBA numerical calculation shows only one strong transition from 4_2^+ to 4_1^+ , the other transitions being much weaker. Based on the qualitatively good description of its properties, one may assign the 4_2^+ state as a member of the ($\xi = 1, \tau = 3$) multiplet of the E(5) model.

In the case of the 3_1^+ state decay, the strongest B(E2) value is that of the $3_1^+ \rightarrow 2_2^+$ transition. Relative to this transition (chosen as 100), the B(E2, $3_1^+ \rightarrow 4_1^+$)

Table 3. Relative excitation energies of the low lying energy states in ^{124}Te , normalized to the energy of the first 2^+ state, compared with the predictions of the symmetry models of Ref. 22. The values in bold face represent the closest model predictions relative to the experimental ones. (See text for discussion.)

Level J^π	Experimental	U(5)	E(5)- β^4	E(5)- β^6	E(5)- β^8	E(5)
2_1^+	1	1	1	1	1	1
4_1^+	2.070	2.000	2.093	2.135	2.157	2.199
2_2^+	2.197	2.000	2.093	2.135	2.157	2.199
0_2^+	2.748	2.000	2.390	2.619	2.756	3.031
6_1^+	2.897	3.000	3.265	3.391	3.459	3.590
0_3^+	3.123	3.000	3.265	3.391	3.459	3.590
4_2^+	3.247	3.000	3.265	3.391	3.459	3.590
3_1^+	3.381	3.000	3.265	3.391	3.459	3.590

Table 4. Relative B(E2) values normalized to the value of the $2_1^+ \rightarrow 0_1^+$ transition, compared with the theoretical predictions of the symmetry models of Ref. 22. The values in bold face represent the closest values to the experimental ones. (See text for discussion.)

Transition $J_i^\pi \rightarrow J_f^\pi$	Experimental B(E2)	U(5)	E(5)- β^4	E(5)- β^6	E(5)- β^8	E(5)
$2_1^+ \rightarrow 0_1^+$	1	1	1	1	1	1
$4_1^+ \rightarrow 2_1^+$	3.133(2133)	2.000	1.832	1.766	1.733	1.674
$2_2^+ \rightarrow 2_1^+$	1.833(74)	2.000	1.832	1.766	1.733	1.674
$3_1^+ \rightarrow 2_2^+$	< 5.200	2.143	1.831	1.713	1.655	1.549
$3_1^+ \rightarrow 4_1^+$	< 0.167	0.857	0.732	0.685	0.662	0.620
$0_3^+ \rightarrow 2_2^+$	12.167(9966)	3.000	2.564	2.398	2.316	2.169
$0_2^+ \rightarrow 2_1^+$	0.633(66)	2.000	1.418	1.190	1.076	0.868

and $B(E2, 3_1^+ \rightarrow 2_1^+)$ values are 37, and 5, respectively. This decay pattern resembles that of the 3_1^+ member of the ($\xi = 1, \tau = 3$) multiplet. Also, the calculated values do not contradict the limits of the absolute experimental values (< 156 W.u. for the $3_1^+ \rightarrow 2_2^+$, < 0.2 W.u. for the $3_1^+ \rightarrow 2_1^+$, and < 5 W.u. for the $3_1^+ \rightarrow 4_1^+$), respectively (Fig. 4).

It has been recently proved (Refs. 21 and 22) that the sequence of β^{2n} potentials with n integer could interpolate the values of nuclear observables between the U(5) and E(5) symmetries. In Tables 3 and 4 we present a comparison of the relative experimental energies and $B(E2)$ values with the U(5), E(5)- β^{2n} ($n = 2, 3, 4$) and E(5) theoretical predictions.

As can be observed from Table 3, some experimental excitation energies (for 4_1^+ , 6_1^+ and 4_2^+ states) are closer to E(5) - β^2 (U(5)) and E(5)- β^4 predictions. Only the energy of the 2_2^+ is better described in the “classical” E(5) limit ($n \rightarrow \infty$). The 0_2^+ and 3_1^+ values are closer to the E(5)- β^8 and E(5)- β^6 predictions, respectively.

The relative $B(E2)$ values presented in Table 4 indicates that the $4_1^+ \rightarrow 2_1^+$, $3_1^+ \rightarrow 2_2^+$ and $0_3^+ \rightarrow 2_2^+$ transitions are best described by the E(5)- β^2 (U(5)) symmetry, and the $2_2^+ \rightarrow 2_1^+$ transition is better reproduced by the E(5)- β^4 predictions. The E(5) symmetry provides the best description for the $3_1^+ \rightarrow 4_1^+$ and $0_2^+ \rightarrow 2_1^+$ transitions.

The present experimental data do not clearly single out one of these refinements of the E(5) model. More accurate experimental data on reduced transition probabilities are needed in order to achieve this goal.

4. Conclusions

In the present work, we have revised the level scheme of ¹²⁴Te as seen from the β^+/ε decay of ¹²⁴I. New experimental information has been added to the previously adopted level decay scheme (three new levels seen for the first time in the β -decay, weak γ -ray decay branches added). Nevertheless, for the lowest collective states, with E_x below 2.1 MeV, our experimental results coincide with the previous ones.² The existing information was tested in detail against model predictions, namely, those of E(5) critical point symmetry and IBA-1 at the critical point of the U(5)-O(6) phase transition. Both the $R_{4/2}$ value and γ -band staggering factor S_4 , as well as the decay properties of the 2_2^+ , 3_1^+ , 4_2^+ , 0_2^+ and 0_3^+ states, firmly point towards a E(5) structure for the ¹²⁴Te nucleus. A clearer assignment of this structure still requires new measurements of absolute values for the transition strengths and weak branching ratios for the γ -decay of the low-lying non-yrast states.

Acknowledgments

The authors thank Dr. Nicolae Marginean for a careful reading of the manuscript and for his useful suggestions. This work was partly supported by the National Authority for Scientific Research through the Research Grants CEx-05-D11-30 and CEx-05-D11-50.

References

1. F. Iachello and A. Arima, *The Interacting Boson Model* (Cambridge University Press, Cambridge, 1987).
2. N. Warr *et al.*, *Nucl. Phys. A* **636** (1998) 379.
3. R. Georgii *et al.*, *Nucl. Phys. A* **592** (1995) 307.
4. J. Rikovska *et al.*, *Nucl. Phys. A* **505** (1989) 145.
5. C. Doll *et al.*, *Nucl. Phys. A* **672** (2000) 3.
6. R. F. Casten, in *Interacting Bose–Fermi Systems in Nuclei*, ed. F. Iachello (Plenum, New York, 1981).
7. S. J. Robinson *et al.*, *J. Phys. G: Nucl. Phys.* **9** (1983) L71.
8. C. S. Lee *et al.*, *Nucl. Phys. A* **530** (1991) 58.
9. F. Iachello, *Phys. Rev. Lett.* **85** (2000) 3580.
10. F. Iachello, *Phys. Rev. Lett.* **87** (2001) 052502.
11. R. F. Casten and N. V. Zamfir, *Phys. Rev. Lett.* **87** (2001) 052503.
12. R. F. Casten and N. V. Zamfir, *Phys. Rev. Lett.* **85** (2000) 3584.
13. N. V. Zamfir *et al.*, *Phys. Rev. C* **65** (2002) 044325.
14. R. M. Clark *et al.*, *Phys. Rev. C* **69** (2004) 064322.
15. C. Mihai *et al.*, *Phys. Rev. C* **75** (2007) 044302.
16. H. Iimura, J. Katakura, K. Kitao and T. Tamura, *Nucl. Data Sheets* **80** (1997) 895.
17. T. von Egidy *et al.*, *Phys. Rev. C* **74** (2006) 034319.
18. A. E. L. Dieperink, O. Scholten and F. Iachello, *Phys. Rev. Lett.* **44** (1980) 1747.
19. G. Suliman, private communication.
20. R. F. Casten *et al.*, *Phys. Rev. C* **44** (1991) 1.
21. J. M. Arias *et al.*, *Phys. Rev. C* **68** (2003) 041302(R).
22. D. Bonatsos *et al.*, *Phys. Rev. C* **69** (2004) 044316.